doi: 10.17221/80/2017-VETMED

# Low-field magnetic resonance imaging for 3D volume rendering of canine stifle joint pathologies: a case report

A. Przeworski*, Z. Adamiak, J. Glodek

University of Warmia and Mazury, Olsztyn, Poland

*Corresponding author: przeworskiadam@gmail.com

**ABSTRACT**: This article presents a case report in which complex deformities of the canine stifle joint were visualised using 3D volume rendering of images acquired in a low-field MRI system. The use of low-field MRI for 3D volume rendering has been described in human medicine, but no such reports are available as yet in veterinary medicine. A two-year-old male mongrel dog (8.5 kg body mass) with an unknown previous history of hindlimb lameness was presented to our clinic. The left stifle joint was hyperextended, slightly enlarged and it showed a limited range of motion. Three-dimensional sequences were used to visualise bones of the stifle joint. Optimal values of in-plane spatial resolution were obtained for small structures. The developed 3D model contributed to our understanding of the spatial localisation of bone deformities in the patient, which was crucial in surgical planning. This report shows that three-dimensional models do significantly enhance the clinical applicability of low-field MRI.

**Keywords**: bone deformities; dog; MRI; musculoskeletal imaging; three-dimensional

Magnetic resonance imaging enables the visualisation of musculoskeletal system components with complex three-dimensional structures by generating successive multiplanar 2D images. Radiologists and surgeons must have sufficient spatial imagination to analyse and interpret the resulting scans (Burstein et al. 2000; Krupa et al. 2007). However, even the most highly skilled medical personnel are not always able to correctly diagnose complex bone deformities. In recent years, remarkable progress has been made in the reconstruction of 3D objects, which has facilitated diagnosis and has improved the quality and accuracy of imaging (Anastasi et al. 2007). This advanced technique supports the development of volumetric models of complex structures based on 2D image slices (Eley et al. 2014).

Volume rendering of the skeletal system is generally based on computed tomography (CT) data, which improves surgical planning and diagnosis, while minimising the invested effort (Eley et al. 2014). MRI volume rendering was used with success to accurately render various structures of the human knee, including bones (Rusinek et al. 1989). Three-dimensional visualisation of MRI data is highly challenging (Moro-oka et al. 2007). Data from MRI scans, in particular those generated by a low-field system, can be used to analyse macrostructures owing to the low spatial and temporal resolution (Udupa 1999; Anastasi et al. 2007).

Magnetic resonance imaging is more suitable for imaging soft tissues, whereas CT has been recommended for bone analysis (Fishman et al. 1987; Adamiak et al. 2011). The potential of both imaging techniques has been harnessed by introducing multimodal imaging which incorporates MRI and CT data. This approach contributes to accurate 3D reconstruction and visualisation of the examined area, and it overcomes the limitations of both imaging methods (Zarucco et al. 2006; Blumenfeld et al. 2008; Lee et al 2008; Markelj et al. 2012).

To our knowledge, skeletal deformations in the canine stifle joint have never before been visualised

doi: 10.17221/80/2017-VETMED

by volume rendering in low-field MRI. Here, we present a case report showing the application of MRI slices in 3D volume rendering of pathological changes in the canine stifle joint.

## Case description

A two-year-old male mongrel dog weighing 8.5 kg was admitted to our clinic. The dog had a problem with movement and did not bear weight on the left hind limb. The duration of lameness was unknown because he had been rescued three months previously. On physical examination, the dog had a slightly enlarged stifle joint, which was hyperextended with a limited range of motion (15°). Distortion could be palpated on the cranio-medial side of the femur. The stifle joint had previously been subjected to a radiographic examination (Siemens, Comet AG CH-3097, 64 kV, 4.0 mAs) in mediolateral and caudocranial projections (Figure 1).

Images were acquired using a low-field magnetic resonance imaging scanner (Vet-MR Grande, Esaote, 0.25T, Italy). The dog was positioned in right lateral recumbency, and the hyperextended stifle joint was placed in the centre of the dual phased array coil. Proper alignment in the coil was provided by cushions attached to the MRI device. Contrast enhancement was not used. The data used in the 3D reconstruction were obtained during a routine clinical examination in a low-field MRI system according to the standard protocol. The examination was performed under general anaesthesia, according to the following standard protocol: medetomidine (50 µg/kg *i.m.*, Ceptor 1 mg/ml, ScanVet, Poland) followed by propofol (2–4 mg/kg *i.v.*, Scanofol, 10 mg/ml, ScanVet, Poland) and maintained with intravenous infusion of propofol (0.3 mg/kg/min *i.v.*, Scanofol, 10 mg/ml, ScanVet, Poland) using an infusion pump (B. Braun's Perfusor® Space Infusion Pump).

The Spin Echo T1 3D HF (TR = 300 ms, TE = 24 ms, NEX = 1, matrix = 192 × 116 × 18, FOV = 170 × 130 × 60, flip angle = 90°, slice thickness = 1.9 mm, time = 6:20) 3D sequence was used for volume rendering on account of satisfactory post-processing results (Figure 2).

In the next stage of the procedure, data were exported to DICOM (Digital Imaging and Communications in Medicine). Data were processed in the 3DSlicer 4.5.0-1 application (http://www.slicer.org) (Fedorov et al. 2012) which supports interactive visualisation and analysis (registration or segmentation) of various medical images (CT, MRI, ultrasonography). We focused on unusual MRI findings in order to visualise bone structures in the pathologically changed areas.

In each slice, bones were distinguished from surrounding tissues in the segmentation procedure. The first procedure involved an interactive thresholding tool which supports quick and automatic data processing. The software automatically classifies individual pixels as respective tissues which are characterised by different degrees of accuracy depending on the quality of the source image. Manual adjustments were introduced for contour-based segmentation of objects aligned with the bone

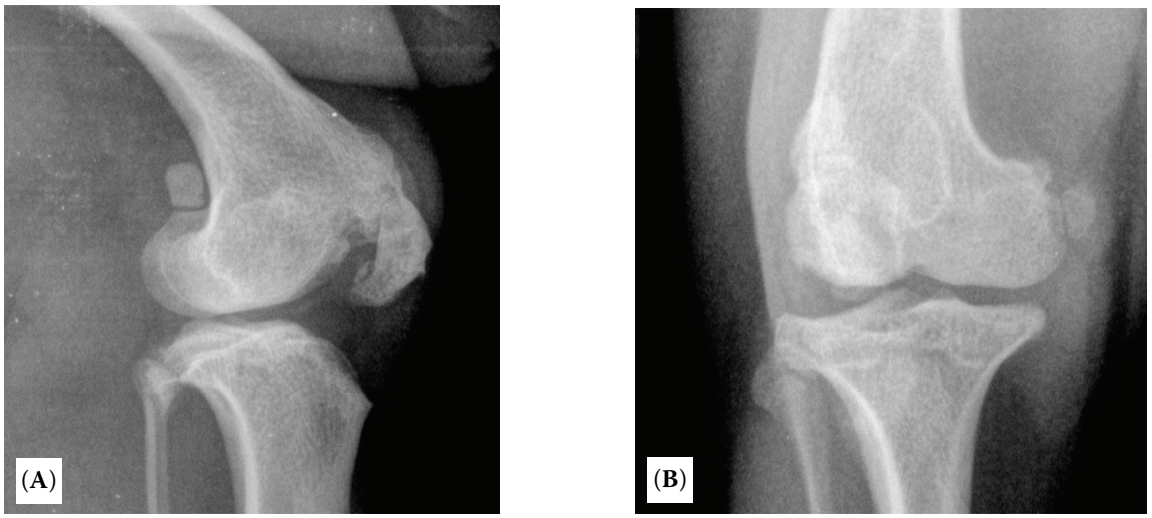


Figure 1. Radiographs of a stifle joint in mediolateral (**A**) and caudocranial (**B**) projections

doi: 10.17221/80/2017-VETMED

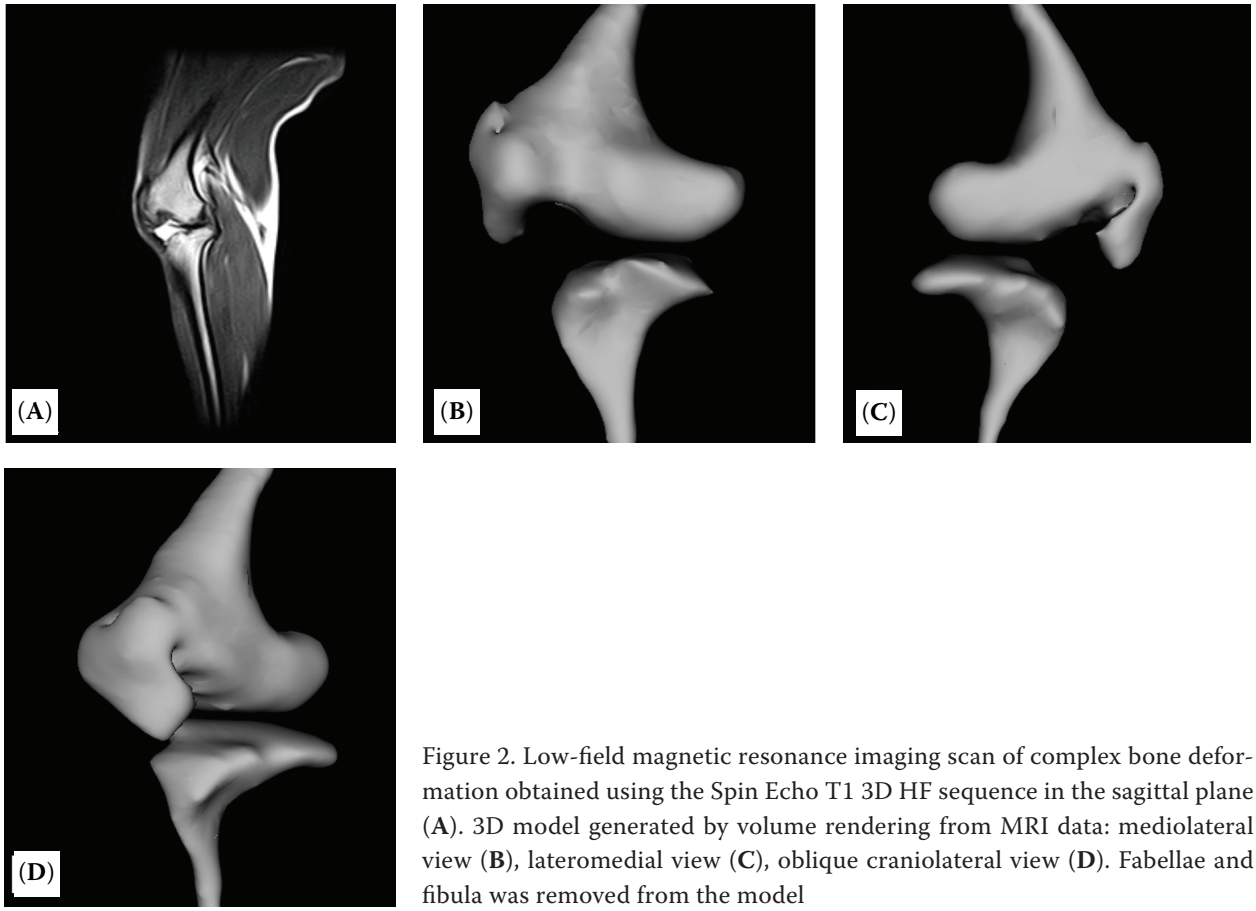


Figure 2. Low-field magnetic resonance imaging scan of complex bone deformation obtained using the Spin Echo T1 3D HF sequence in the sagittal plane (**A**). 3D model generated by volume rendering from MRI data: mediolateral view (**B**), lateromedial view (**C**), oblique craniolateral view (**D**). Fabellae and fibula was removed from the model

boundary. A volumetric 3D model was generated by volume rendering. Finally, the 3D model was cropped to the region of interest to eliminate distraction from the main focus (Figure 2).

## DISCUSSION AND CONCLUSIONS

This case presented the applicability of 3D reconstruction for identifying pathological changes in the stifle joint of a canine patient, based on data generated in a low-field MRI system. While the model contributed to an understanding of the relationships between bone distortions and their spatial location, the obtained radiographs did not allow accurate interpretation of deformation due to overlapping structures of the bone in standard projections.

MRI has been used for the purpose of generating different 3D models from soft tissues. Rusinek et al. (1989) used a similar technique for 3D reconstruction of the human brain, hepatic portal veins and the knee based on data acquired in a 0.5T MRI system. In examinations of the knee, dedicated algorithms were used to reconstruct structures with low signal intensity, such as menisci and ligaments. Technological limitations meant that, at that time, the relevant procedures were highly time-consuming. High-field MRI data were also used in a stereo 3D reconstruction of the anatomical structures of a normal human ankle and knee, which supported accurate evaluations of tendons, muscles, bones and cartilages (Anastasi et al. 2007; Anastasi et al. 2009).

Three-dimensional reconstruction has evolved into 3D geometrical modelling as an accurate method for simulating and planning or training for computer-aided surgery (Krupa et al. 2007; Loke et al. 2017; Oshiro and Ohkohchi 2017). For a better understanding or for analysis, the obtained model could be rotated, and the superimposed objects could be switched on and off and cropped. Moreover, colouring the region of interest or modifying it by changing the transparency of selected structures could further enhance the model, which can be developed with the use of a 3D printer, and then manually modified by the surgeon in preparation for the surgery.

doi: 10.17221/80/2017-VETMED

The applicability of MRI-based 3D models for educational purposes, diagnostic decision making and scientific research has recently been demonstrated. Three-dimensional volume modelling can also compensate for the shortage of cadavers for dissection in medical education (Anastasi et al. 2007; Pedoia et al. 2015).

Computed tomography scans are currently the gold standard of acquiring data for 3D models of the bone. We realize that CT scans would be a more appropriate source of data, but in the analysed case, 3D volume rendering was performed as part of the MRI examination of the canine stifle joint. The obtained bone model was based on the contour of the bone marrow, because the cortical bone is not visible on the MRI. Rathnayaka et al. (2012) determined that long bone models obtained from MRI-based data did not differ statistically from those obtained with CT.

The three-dimensional sequence which supports the acquisition of signal from the entire volume of the stifle joint was used. The deployed sequence produced thick slices without gaps, which is required in low-field MRI for imaging fine structures in small dogs (reduced partial volume averaging). The duration of the 3D sequence is generally longer in comparison with the corresponding 2D sequence. Anastasi et al. (2009) avoided this sequence due to potential motion artefacts. In our study, all procedures were performed under general anaesthesia, which eliminated the risk of motion artefacts.

Obtaining an acceptable model that reliably renders the analysed object is a time-consuming process. The data acquired during the MRI examination included noise and other artefacts; therefore, segmentation could not be fully automated. This applies particularly to the proximal and distal end of the bone due to the overlap of signal intensities between the bones and the adjacent tissues such as ligaments, tendons, muscles, fat and cartilage (Rathnayaka et al. 2012). Moreover, small, ill-defined structures could be difficult to visualise due to the loss of information during the process, potentially necessitating manual correction (Anastasi et al. 2007). All manual adjustments must be performed by a person capable of verifying the segmentation area to minimise the loss of digital image integrity and to avoid minor discontinuities during segmentation. In order to obtain a 3D model with a high geometric accuracy, the person performing the modelling should be familiar with anatomy in order that errors in bone boundary determination are kept to a minimum (Lee et al. 2008; Anastasi et al. 2009; Rathnayaka et al. 2012). Similar observations were made during segmentation of CT data (Rathnayaka et al. 2010; Rathnayaka et al. 2012). In our case, approximately 70% of the surgical procedures were performed automatically. The overall time for visualising the rendered object was approximately 60 min.

MRI-based volume rendering is an excellent non-ionising tool for mapping the spatial localisation of nearly all structures in the body. In this case report, we attempted to evaluate the possibility of 3D reconstruction based on low-field MRI data, with satisfactory results. The described method can be used to increase imaging accuracy and shorten the time to diagnosis. Further research is required to maximise the applicability of volume rendering in clinical practice.

## REFERENCES

Adamiak Z, Jaskolska M, Matyjasik H, Pomianowski A, Kwiatkowska M (2011): Magnetic resonance imaging of selected limb joints in dogs. Polish Journal of Veterinary Sciences 14, 501–505.

Anastasi G, Bramanti P, Di Bella P, Favaloro A, Trimarchi F, Magaudda L, Gaeta M, Scribano E, Bruschetta D, Milardi D (2007): Volume rendering based on magnetic resonance imaging: advances in understanding the three-dimensional anatomy of the human knee. Journal of Anatomy 211, 399–406.

Anastasi G, Cutroneo G, Bruschetta D, Trimarchi F, Ielitro G, Cammaroto S, Duca A, Bramanti P, Favaloro A, Vaccarino G, Milardi D (2009): Three-dimensional volume rendering of the ankle based on magnetic resonance images enables the generation of images comparable to real anatomy. Journal of Anatomy 215, 592–599.

Blumenfeld J, Studholme C, Carballido-Gamio J, Carpenter D, Link TM, Majumdar S (2008): Three-dimensional image registration of MR proximal femur images for the analysis of trabecular bone parameters. Medical Physics 35, 4630–4639.

Burstein D, Bashir A, Gray ML (2000): MRI techniques in early stages of cartilage disease. Investigative Radiology 35, 622–638.

Eley KA, Watt-Smith SR, Sheerin F, Golding SJ (2014): "Black Bone" MRI: a potential alternative to CT with three-dimensional reconstruction of the craniofacial skel-

doi: 10.17221/80/2017-VETMED

eton in the diagnosis of craniosynostosis. European Radiology 24, 2417–2426.

Fedorov A, Beichel R, Kalpathy-Cramer J, Finet J, Fillion-Robin JC, Pujol S, Bauer C, Jennings D, Fennessy F, Sonka M, Buatti J, Aylward S, Miller JV, Pieper S, Kikinis R (2012): 3D Slicer as an image computing platform for the Quantitative Imaging Network. Magnetic Resonance Imaging 30, 1323–1341.

Fishman EK, Drebin B, Magid D, Scott WW, Ney DR, Brooker AF, Riley LH, St Ville JA, Zerhouni EA, Siegelman SS (1987): Volumetric rendering techniques: Applications for three-dimensional imaging of the hip. Radiology 163, 737–738.

Krupa P, Krsek P, Javornik M, Dostal O, Srnec R, Usvald D, Proks P, Kecova H, Amler E, Jancar J, Gal P, Planka L, Necas A (2007): Use of 3D geometry modeling of osteochondrosis-like iatrogenic lesions as a template for press-and-fit scaffold seeded with mesenchymal stem cells. Physiological Research 56 Suppl 1, S107–S114.

Lee Y, Seon J, Shin V, Kim GH, Jeon M (2008): Anatomical evaluation of CT-MRI combined femoral model. Biomedical Engineering Online 7, doi: 10.1186/1475-925X-7-6.

Loke YH, Harahsheh AS, Krieger A, Olivieri LJ (2017): Usage of 3D models of tetralogy of Fallot for medical education: impact on learning congenital heart disease. BMC Medical Education 17, doi: 10.1186/s12909-017-0889-0.

Markelj P, Tomazevic D, Likar B, Pernus F (2012): A review of 3D/2D registration methods for image-guided interventions. Medical Image Analysis 16, 642–661.

Moro-oka TA, Hamai S, Miura H, Shimoto T, Higaki H, Fregly BJ, Iwamoto Y, Banks SA (2007): Can magnetic resonance imaging-derived bone models be used for accurate motion measurement with single-plane three-dimensional shape registration? Journal of Orthopaedic Research 25, 867–872.

Oshiro Y, Ohkohchi N (2017): Three-dimensional liver surgery simulation: Computer-assisted surgical planning with three-dimensional simulation software and three-dimensional printing. Tissue Engineering Part A 23, 474–480.

Pedoia V, Lansdown DA, Zaid M, McCulloch CE, Souza R, Ma CB, Li X (2015): Three-dimensional MRI-based statistical shape model and application to a cohort of knees with acute ACL injury. Osteoarthritis Cartilage 23, 1695–1703.

Rathnayaka K, Sahama T, Schuetz MA, Schmutz B (2010): Effects of CT image segmentation methods on the accuracy of long bone 3D reconstructions. Medical Engineering and Physics 33, 226–233.

Rathnayaka K, Momot KI, Noser H, Volp A, Schuetz MA, Sahama T, Schmutz B (2012): Quantification of the accuracy of MRI generated 3D models of long bones compared to CT generated 3D models. Medical Engineering and Physics 34, 357–363.

Rusinek H, Mourino MR, Firooznia H, Weinreb JC, Chase NE (1989): Volumetric rendering of MR images. Radiology 171, 269–272.

Udupa JK (1999): Three-dimensional visualization and analysis methodologies: a current perspective. Radiographics 19, 783–806.

Zarucco L, Wisner ER, Swanstrom MD, Stover SM (2006): Image fusion of computed tomographic and magnetic resonance images for the development of a three-dimensional musculoskeletal model of the equine forelimb. Veterinary Radiology and Ultrasound 47, 553–562.

Received: December 7, 2016
Accepted after corrections: September 29, 2017